ACCOUNTS
of chemical research

Theranostic Nanomedicine

TWAN LAMMERS,[*,†,‡,§] SILVIO AIME,[∥] WIM E. HENNINK,[‡] GERT STORM,[‡,⊥] AND FABIAN KIESSLING[†,⊥]

[†]*Department of Experimental Molecular Imaging, Helmholtz Institute for Biomedical Engineering, RWTH - Aachen University, Pauwelsstrasse 20, 52074 Aachen, Germany,* [‡]*Department of Pharmaceutics, Utrecht Institute for Pharmaceutical Sciences, Utrecht University, Sorbonnelaan 16, 3584 CA Utrecht, The Netherlands,* [§]*Department of Innovative Cancer Diagnosis and Therapy, Clinical Cooperation Unit Radiation Oncology, German Cancer Research Center, Im Neuenheimer Feld 280, 69120 Heidelberg, Germany, and* [∥]*Department of Chemistry IFM and Molecular Imaging Center, University of Torino, Via P. Giuria 7, 10125 Torino, Italy*

RECEIVED ON JANUARY 27, 2011

CONSPECTUS

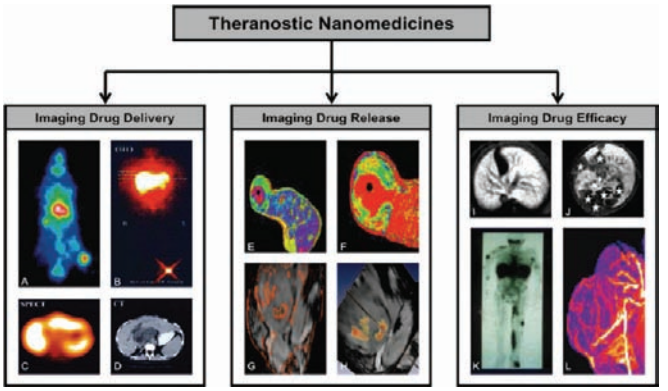

Nanomedicine formulations aim to improve the biodistribution and the target site accumulation of systemically administered (chemo)therapeutic agents. Many different types of nanomedicines have been evaluated over the years, including for instance liposomes, polymers, micelles and antibodies, and a significant amount of evidence has been obtained showing that these submicrometer-sized carrier materials are able to improve the balance between the efficacy and the toxicity of therapeutic interventions. Besides for therapeutic purposes, nanomedicine formulations have in recent years also been increasingly employed for imaging applications. Moreover, paralleled by advances in chemistry, biology, pharmacy, nanotechnology, medicine and imaging, several different systems have been developed in the last decade in which disease diagnosis and therapy are combined. These so-called (nano) theranostics contain both a drug and an imaging agent within a single formulation, and they can be used for various different purposes.

In this Account, we summarize several exemplary efforts in this regard, and we show that theranostic nanomedicines are highly suitable systems for monitoring drug delivery, drug release and drug efficacy. The (pre)clinically most relevant applications of theranostic nanomedicines relate to their use for validating and optimizing the properties of drug delivery systems, and to their ability to be used for pre-screening patients and enabling personalized medicine. Regarding the former, the combination of diagnostic and therapeutic agents within a single formulation provides real-time feedback on the pharmacokinetics, the target site localization and the (off-target) healthy organ accumulation of nanomedicines. Various examples of this will be highlighted in this Account, illustrating that by non-invasively visualizing how well carrier materials are able to deliver pharmacologically active agents to the pathological site, and how well they are able to prevent them from accumulating in potentially endangered healthy tissues, important information can be obtained for optimizing the basic properties of drug delivery systems, as well as for improving the balance between the efficacy and the toxicity of targeted therapeutic interventions. Regarding personalized medicine, it can be reasoned that only in patients which show high levels of target site accumulation, and which respond well to the first couple of treatment cycles, targeted therapy should be continued, and that in those in which this is not the case, other therapeutic options should be considered. Based on these insights, we expect that ever more efforts will be invested in developing theranostic nanomedicines, and that these systems and strategies will contribute substantially to realizing the potential of personalized medicine.

Published on the Web 05/05/2011 www.pubs.acs.org/accounts
10.1021/ar200019c

Introduction

Nanomedicines are submicrometer-sized carrier materials designed to improve the biodistribution of systemically administered (chemo)therapeutic agents. Clinically relevant examples of nanomedicine formulations are liposomes, polymers, micelles, solid (lipid) nanoparticles, and antibodies. By delivering pharmacologically active agents more effectively and more selectively to the pathological site (site-specific drug delivery) and/or by guiding them away from potentially endangered healthy tissues (site-avoidance drug delivery), nanomedicines aim to improve the balance between the efficacy and the toxicity of systemic (chemo)therapeutic interventions.[1−4]

Besides for drug targeting to pathological sites and for therapeutic purposes, nanomedicine formulations have also been more and more used for imaging applications as well as, in recent years, for theranostic approaches, that is, for systems and strategies in which disease diagnosis and therapy are combined.[5−8] To this end, on the one hand, "classical" drug delivery systems, such as liposomes, polymers, micelles, solid (lipid) nanoparticles, and antibodies, are being co-loaded both with drugs and with contrast agents (Figure 1). On the other hand, also nanomaterials with an intrinsic ability to be used for imaging purposes, such as gold- and iron oxide-based nanoparticles, are increasingly being loaded with drugs and implemented for combining disease diagnosis and therapy.

Based on the advances made in, and the close collaboration between, several different scientific disciplines, such as chemistry, biology, pharmacy, nanotechnology, medicine, and imaging, ever more of such theranostic nanomedicines have been designed and evaluated over the past few years, and ever more interesting applications are being envisioned for nanotheranostics (Figures 2 and 3). In the present Account, we summarize several exemplary efforts in this regard, and we show that theranostic nanomedicines are highly suitable systems for monitoring drug delivery, drug release, and drug efficacy.

Imaging Drug Delivery

As already briefly outlined above, nanomedicine formulations are primarily designed to improve the biodistribution and the target site accumulation of systemically administered (chemo)therapeutic agents. To facilitate pharmacokinetic and biodistributional analyses, and to thereby improve drug targeting to pathological sites, it would be highly useful if the circulation time and the organ accumulation of nanomedicine formulations could be visualized noninvasively in real-time. To achieve this goal, many different types of nanomedicines have been co-loaded both with drugs and with imaging agents.

In the majority of cases, radionuclides have been used for such purposes. Large numbers of radionuclide-labeled liposomes, polymers, micelles, nanoparticles, and antibodies have been subjected to biodistribution analyses over the years, both in animal models and in patients, and it has become clear that such studies substantially assist in improving our understanding of the drug delivery process, as well as in predicting the therapeutic potential of (tumor-) targeted nanomedicines.

Figure 3A−D provides an overview of several exemplary efforts in this regard. Figure 3A shows that iodine-131-labeled HPMA (i.e., *N*-(2-hydroxypropyl)methacrylamide) copolymers can be used to visualize the biodistribution of long-circulating and passively tumor-targeted polymeric drug carriers in rats bearing subcutaneously transplanted Dunning AT1 tumors. Using such radiolabeled copolymers, it has for instance been demonstrated that in line with the principles of enhanced permeability and retention- (EPR-) mediated passive drug targeting,[9] higher molecular weight HPMA copolymers circulate for significantly longer periods of time than do lower molecular weight copolymers and consequently accumulate in tumors significantly more effectively.[10] In a similar setup, it has been demonstrated that the physicochemical modification of HPMA copolymers, e.g., with

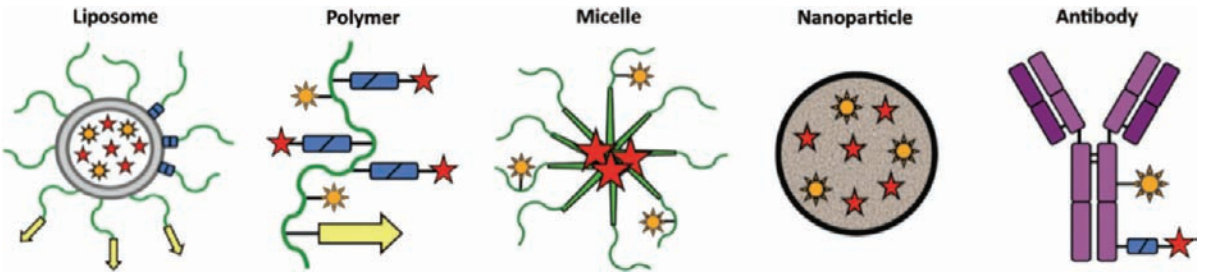

FIGURE 1. Theranostic nanomedicines. Liposomes and liposomal bilayers are shown in gray; polymers and polymer-coatings in green; solid (lipid) nanoparticle components in brown; antibodies in purple; linkers allowing for drug release and for sheddable stealth coatings in blue; targeting ligands in yellow; imaging agents in orange; and conjugated or entrapped pharmacologically active agents in red.

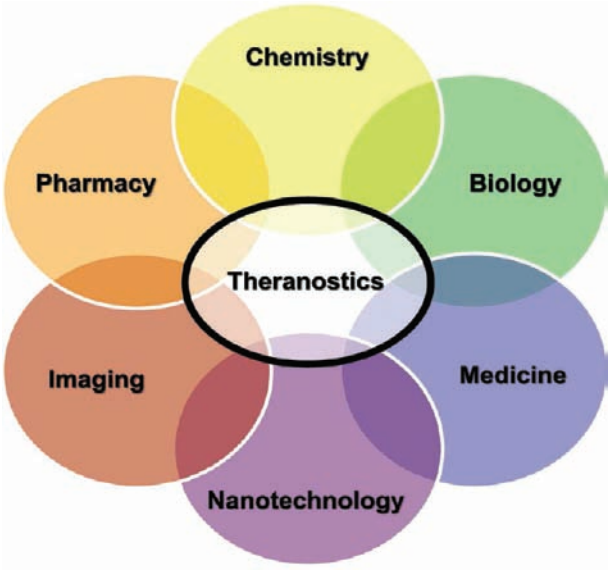

FIGURE 2. Theranostics. Schematic representation of the highly interdisciplinary field of (nano)theranostics. Theranostics are nanomedicine formulations which aim to combine disease diagnosis (in its broadest sense; including patient prescreening and therapy monitoring) and therapy, and which are developed and tested by researchers working at the intersection of several different scientific fields.

positively or negatively charged groups, as well their functionalization with drugs, with drug linkers and with targeting peptides, reduces the long-circulating properties of the copolymers, but that it does not negatively affect their tumor-targeting potential: both unfunctionalized and functionalized HPMA copolymers accumulated in tumors significantly more effectively than in 6−8 out of 9 healthy tissues.[11]

Figure 3B−D shows the biodistribution and the target site accumulation of a radionuclide-labeled liver-targeted HPMA copolymer carrying doxorubicin (i.e., PK2). This theranostic nanomedicine formulation was targeted to the liver using galactosamine (which binds to the asialoglycoprotein receptor, which is overexpressed on hepatocytes), and effective organ targeting could be clearly visualized using 2-D gamma-scintigraphy (Figure 3B).[12] When looking in more detail at the efficacy of drug targeting at the organ level, however, using anatomical CT imaging and functional SPECT imaging, it was found that the majority of PK2 ended up in healthy liver, rather than in the tumorous areas of the liver (Figure 3C,D), thereby demonstrating that this formulation was not very effective in selectively delivering the conjugated drug to the pathological site.

In a comparable experimental setup, Harrington and colleagues evaluated the biodistribution and the target site accumulation of indium-111-labeled PEGylated liposomes in 17 patients suffering from various different types of malignancy (i.e., breast, head and neck, lung, brain, and cervical cancer).[13] As exemplified by Figure 4, they showed that PEGylated liposomes circulate for prolonged periods of time, with an average $t_{1/2\beta}$ of 76 h, and with more than 50% of the injected dose still present in systemic circulation at 48 h post i.v. injection (p.i.). In addition, they showed that the radiolabeled liposomes effectively localized to tumors in 15 out of 17 cases, with the overall levels of liposome uptake varying from ~0.5 to ~3.5% of the injected dose at 72 h p.i., and with the degree of tumor accumulation closely correlating with the type of malignancy (Figure 4I): the highest level of uptake was found for head and neck cancer (33 ± 16%ID/kg tumor; Figure 4A−D), and the lowest level for breast cancer (5 ± 3%ID/kg tumor; Figure 4E−G). Interestingly, in case of the latter, in spite of relatively low overall tumor concentrations, it was observed that the radiolabeled liposomes effectively accumulated in axillary lymph nodes (Figure 4G), which are typically employed by breast cancers to metastasize. Significant accumulation of the radiolabeled liposomes was also observed in organs of the reticulo-endothelial system (RES), like liver and spleen, which are known to be involved in the clearance of long-circulating nanomedicines from the circulation (Figure 4A, E−G). Such image-guided insights into the efficacy of liposome-mediated drug targeting are considered to be highly useful for prescreening patients assigned to, e.g. Doxil (i.e., PEGylated liposomal doxorubicin), in order to identify which tumors are amenable to EPR-mediated drug targeting and which are not, and to thereby predict which patients are likely to respond to therapy and which are not.

An important downside of the pioneering work by Harrington and colleagues is that the liposomes they used did not contain a drug.[13] It is important to take into account in this regard that it is very likely that there are significant differences in the pharmacokinetics, the biodistribution, and the target site localization of drug-free "nanodiagnostics" versus drug-containing "nanotheranostics". This not only because the presence of a pharmacologically active agent can substantially affect the mode and/or the kinetics of clearance, but also because the incorporation of a drug can have major effects on the physicochemical properties of the formulation. Regarding the latter, it has, e.g. been shown that, upon conjugating doxorubicin and gemcitabine to iodine-131-labeled HPMA copolymers, because of altered physicochemical properties, the circulation time of the formulation decreases, while the levels localizing to kidney substantially increase.[14] Regarding the mode and/or the kinetics of clearance, the functionality of the RES needs to

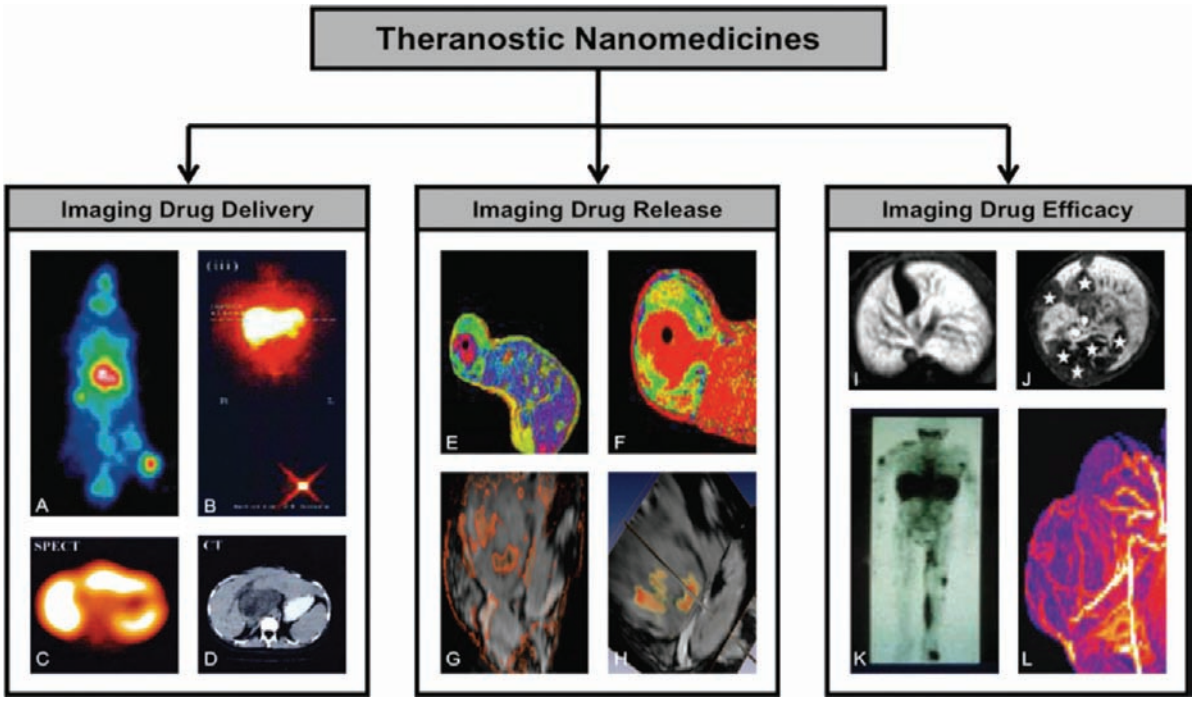

FIGURE 3. Applications of theranostic nanomedicine formulations. Theranostic nanomedicines can be applied for various different purposes, most notably for imaging drug delivery (A–D), drug release (F–H), and drug efficacy (I–L). (A) Gamma camera imaging of the biodistribution and the tumor accumulation of a passively tumor-targeted iodine-131-labeled HPMA copolymer in a Copenhagen rat bearing a Dunning AT1 tumor in its right hind limb. (B) Gamma camera image showing effective active drug targeting to the liver using an iodine-123-labeled galactosamine-modified HPMA copolymer containing doxorubicin (i.e., PK2) in a patient suffering from hepatocellular carcinoma. (C,D) Functional SPECT imaging (C) of the tumor and liver localization of iodine-123-labeled PK2 combined with anatomical CT imaging (D), exemplifying that the majority of the liver-targeted polymeric prodrug does not localize to the (dark) tumorous region in the middle of the SPECT and CT image. (E,F) MR-based visualization and quantification of manganese and doxorubicin release from temperature-sensitive liposomes (TSL). The color-coded Mn^{2+}-enhanced T_1 map obtained at 45 min after the i.v. injection of TSL into a rat bearing a preheated fibrosarcoma tumor is shown in (E). (F) Amount of released doxorubicin calculated and correlated on a pixel-by-pixel basis from the image in (E), exemplifying release in the periphery of the tumor. (G,H) Release of Gd-DTPA from PLGA-based nanoparticles containing SPIO, Gd-DTPA and 5-FU. (G) Subtraction image of precontrast minus postcontrast T_1-map (in red; showing Gd-DTPA release; note that the Gd-DTPA-signal is quenched in close proximity to SPIO), overlaid on a T2*-weighted image, showing the tumor accumulation of the particles (in black). (H) A 3D image depicting T2*-weighted signals overlaid with quantitative T_1 values (yellow, 50 μM; red, 500 μM), enabling quantification of drug release. (I,J) Accumulation of Gd-labeled polypropylene diaminobutane dendrimers in a healthy mouse liver (I) and in a liver containing several metastatic lesions (J), exemplifying the suitability of these particles to visualize liver metastases. (K) Biodistribution of indium-111-labeled PEGylated liposomes in a Kaposi sarcoma patient. Localization to a large tumorous mass in the lower left leg and to several metastatic lesions can be clearly observed, exemplifying the possibility of such formulations for predicting and monitoring treatment responses. (L) Maximal intensity projection of an MR angiography scan of a Dunning AT1 tumor obtained at 30 min after the i.v. injection of a 25 kDa sized gadolinium-labeled HPMA copolymer. Such MR angiography-based approaches are considered to be highly useful for noninvasively assessing the efficacy of nanomedicine-based antiangiogenic interventions. Images adapted with permission from refs 13, 17, 23, 27, and 28.

be taken into account. Without a drug, it is likely that the majority of radiolabeled liposomes or polymers eventually end up in macrophages. In the case of radiolabeled nanomedicines containing a drug (i.e., true nanotheranostics), on the other hand, it is likely that a significant portion of the circulating and/or tumor-associated macrophages are killed by the conjugated or entrapped chemotherapeutic drug, thereby substantially affecting the pharmacokinetics, the organ distribution, and the target site accumulation of the formulation. Because of the accelerated blood clearance (ABC) phenomenon, for instance, radiolabeled PEGylated liposomes are known to be cleared very rapidly from systemic circulation when administered repeatedly to the same animal (within a certain time frame; i.e., up to 3 weeks after the first i.v. injection) and to primarily accumulate in the liver.[15] In the case of doxorubicin-containing PEGylated liposomes, on the other hand, the ABC phenomenon turned out to be absent (because doxorubicin kills (some of) the macrophages responsible for rapid clearance), no decreases in circulation time were observed, and no increases in liver uptake were detected. This observation strongly suggests that by attenuating macrophage uptake and macrophage-mediated clearance, doxorubicin assists in providing long-circulating nanomedicines with proper passive targeting

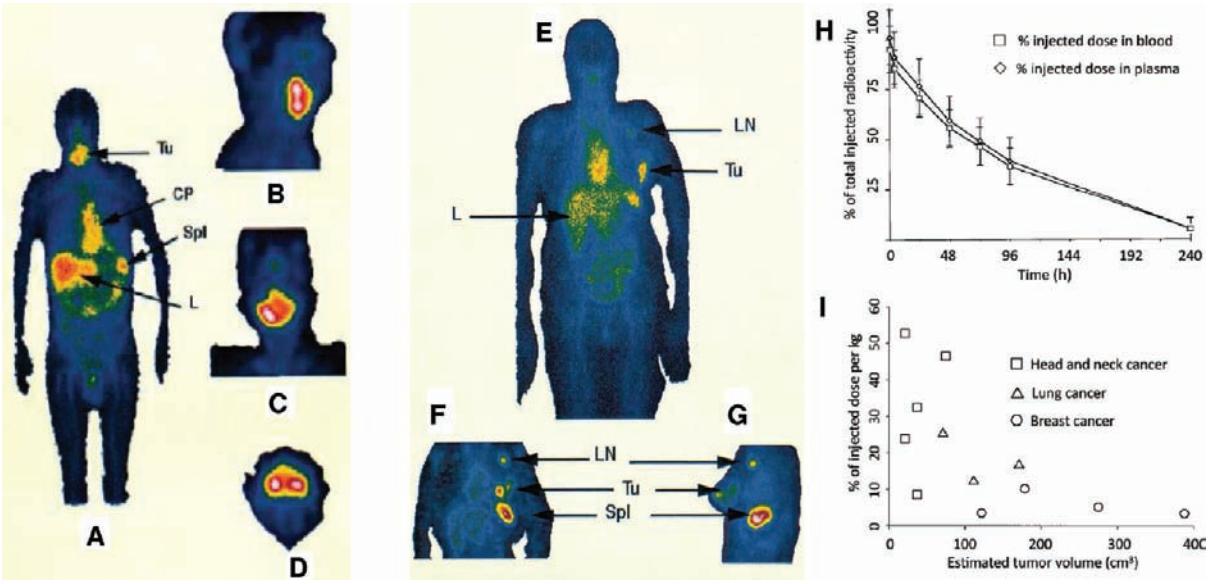

FIGURE 4. Noninvasive imaging of drug delivery. (A–G) Gamma camera images showing the biodistribution of indium-111-labeled PEGylated liposomes at 72 h after i.v. injection into a grade 3 squamous cell carcinoma (A–D) and a grade 4 ductal breast carcinoma (E–G) patient. (A–D) In the SCC patient, it can be seen that, even after 3 days, a substantial amount of the liposomes is still present in systemic circulation (i.e., in the cardiac blood pool; CP), while a significant amount has also already accumulated at the target site (i.e., in a tumor localized at the tongue base; Tu). Significant accumulation was also observed in organs of the reticulo-endothelial system, like liver (L) and spleen (Spl), which are known to be involved in the clearance of long-circulating nanomedicines. (E–G) In the DBC patient, besides localization to blood, tumor (Tu), liver (L), and spleen (Spl), also accumulation in left axillary lymph node (LN) could be clearly observed, indicative of metastasis and of effective drug targeting to this pathological site. (H,I) Besides for assessing target site accumulation, theranostic nanomedicines are also highly useful for analyzing pharmacokinetics (H), as well as for prescreening patients and identifying tumor types (and sizes) amenable to EPR-mediated drug targeting (I). Images adapted with permission from ref 13.

capabilities. Such insights are highly relevant for better understanding and optimizing the efficacy of targeted therapeutic interventions, and they underline the importance of using both drugs and imaging agents within a single formulation when intending to obtain really relevant results with regard to the noninvasive assessment of the biodistribution and the target site accumulation of nanomedicines.

Imaging Drug Release

To enable effective therapy, besides accumulating at the pathological site, the drug also needs to be efficiently released. Since drug release patterns greatly vary from formulation to formulation, and since there are large differences in the release patterns of, for example, liposomes versus polymers versus micelles, it is of the utmost importance to visualize and analyze drug release, not only under semiartificial in vitro conditions but also under physiologically relevant in vivo conditions. In vitro, drug release can generally be analyzed relatively easily, for example, using HPLC, but in vivo this is much more complicated: after harvesting the target tissue, for instance, the material generally needs to be homogenized, and the cells need to be lysed, in order to release the agents from certain intracellular compartments. During these processing steps, and especially during cell lysis (using detergents), many types of carrier materials are destabilized, and, for example, in the case of liposomes, it then is impossible to discriminate between the amount of drug that was still present within liposomes at the point of harvesting and the amount that was already released into the extra- and intracellular environment.

To overcome this shortcoming, and to enable noninvasive in vivo analyses on (the kinetics of) drug release, theranostic nanomedicine formulations have been developed in which drugs and imaging agents are co-loaded into the same delivery system. Since radionuclides render similar signals both in bound/entrapped form and in unbound/free form, these imaging agents are not suitable for visualizing drug release. Magnetic resonance (MR) contrast agents, on the other hand, such as gadolinium and manganese, depend on the interaction with surrounding water molecules to generate a signal, and since this interaction varies substantially when these agents are present within versus outside of water-impermeable vesicles, such as liposomes, MR probes are highly useful materials for monitoring drug release.

Pioneering work in this regard has been performed by Dewhirst and colleagues, who used manganese sulfate not

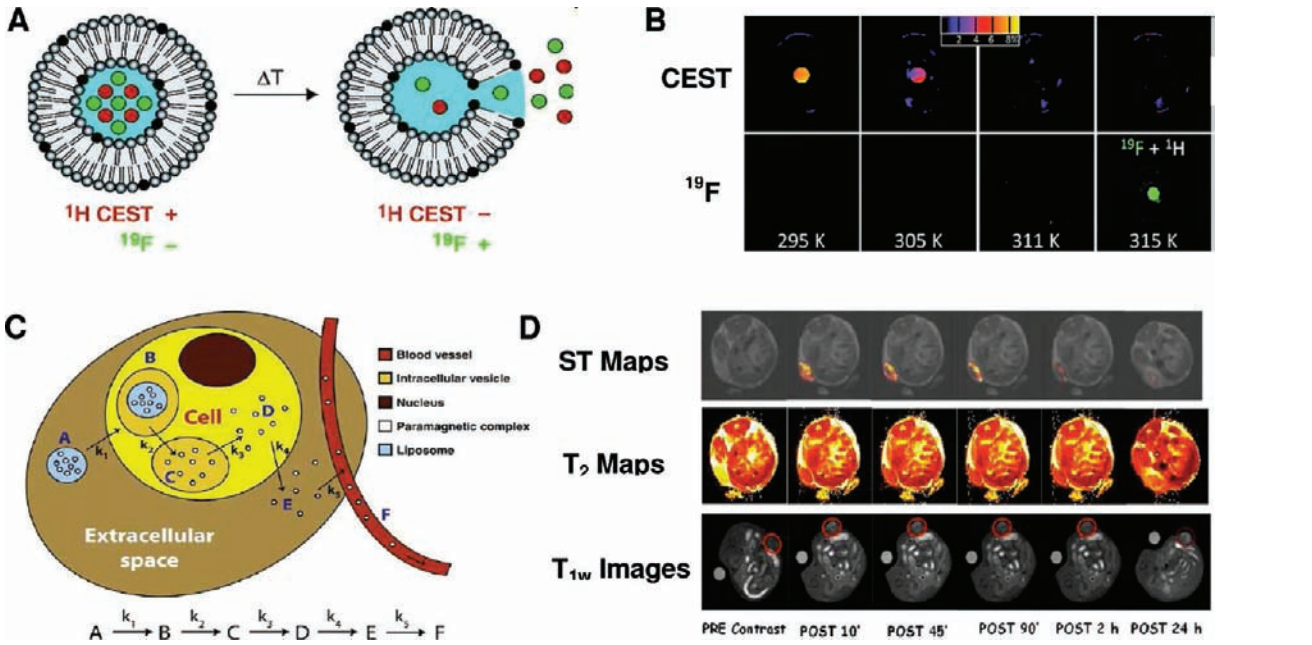

FIGURE 5. Noninvasive imaging of drug release. (A) Schematic depiction of a bimodal temperature-sensitive liposomal (TSL) MR contrast agent enabling the simultaneous visualization of target site accumulation (via a ^{1}H CEST agent; i.e., [Tm(HPDO3A)(H2O)]) and of hyperthermia-induced triggered drug release (via ^{19}F MRI). (B) ^{1}H CEST and ^{19}F MR images of TSL on a clinical 3.0 T MRI scanner. The CEST signal vanished close to T_g of the TSL (i.e., at 311 K; 38 °C), while the fluorine signal appeared at 315 K (i.e., at 42 °C). (C) Schematic representation of the kinetic model used for the analysis of the temporal evolution of three different MR signals upon the intratumoral administration of liposomes containing the T1 contrast agent Gd-HP-DO3A or the CEST agent Tm-DOTMA. The model is based on five consecutive steps, i.e., (i) cellular uptake of intact paramagnetic liposomes from the extracellular space (stage A) by endocytosis into intracellular vesicles (stage B); (ii) desintegration of the liposomal membrane and content release into endo/lysosomal compartments (stage C); (iii) release of the imaging agents from endo/lysosomes into the cytosol (stage D); (iv) cellular efflux of the contrast agents into the extracellular space (stage E); and finally (v) washout of the probes from the extracellular space in the tumor region via the bloodstream (stage F). (D) MR images (obtained at 7 T) illustrating the temporal evolution of the different MR contrast modes and of cellular trafficking of paramagnetic liposomes after intratumoral injection. Images adapted with permission from refs 20 and 22.

only to load doxorubicin into liposomes (by means of a method comparable to ammonium sulfate-based pH-gradient loading) but also to noninvasively visualize drug release (through the generation of an increase in MR signal upon the simultaneous liberation of $MnSO_4$ and doxorubicin). They to this end prepared temperature-sensitive (TSL) and nontemperature-sensitive liposomes (NTSL), and they showed that the relaxivity, that is, the potential for MR signal enhancement, of TSL at temperatures below the transition temperature (T_g) was comparable to that of NTSL, but that it substantially increased upon heating to temperatures exceeding the T_g (i.e., > 39.5 °C), confirming Mn^{2+} release.[16] These findings were corroborated in a follow-up study, in which contrast agent release from TSL was correlated with doxorubicin release, and in which drug dose painting was performed on the basis of MRI,[17] as well as by two recent studies in which doxorubicin release was correlated with ProHance (Gd-HP-DO3A) release.[18,19] As exemplified by Figure 3E and F, TSL rapidly released their contents upon i. v. administration to rats bearing preheated fibrosarcoma tumors, and they primarily did so in the well-vascularized and well-perfused periphery of the tumors.

Langereis, Gruell, and colleagues recently elegantly extended these efforts, developing liposomes containing two different contrast agents, that is, a chemical exchange saturation transfer (CEST) agent and a fluor-19-based probe.[20] As depicted schematically in Figure 5A, the former only generates a signal when the liposomes are intact (and can consequently be used to track the biodistribution of the formulation), and the latter only upon the release of both contrast agents from the liposome (because of "quenching" of the ^{19}F-signal by the paramagnetic CEST agent). The suitability of this agent for visualizing drug release was again demonstrated by preparing temperature-sensitive liposomes, with a T_g of 39 °C. At physiological temperature, the liposomes maintained their integrity and produced a relatively strong CEST signal, while the fluorine signal could not be detected (Figure 5B). At 42 °C, on the other hand, the CEST signal had completely disappeared, and the fluorine signal had become apparent. Such conceptual advances are

considered to be highly important for furthering the clinical development of MR-guided high-intensity focused ultrasound,[21] which is currently only used to treat uterine fibroids but which, because of its ability to heat deep-seated tumors also holds significant potential for implementation in combination with chemotherapy-containing thermosensitive nanotheranostics.

A comparably elegant approach to visualize content release from liposomes has recently been reported by Delli Castelli and colleagues, who used two different types of paramagnetic liposomes, three different MR techniques, and mathematical modeling to kinetically analyze cellular uptake and cellular trafficking upon intratumoral injection.[22] As exemplified by Figure 5C, they subdivided the fate of intratumorally injected paramagnetic liposomes into six different phases, that is, an initial extracellular localization (stage A), uptake into endocytic vesicles, such as endo- and lysosomes (stage B), release of the MR contrast agents in endo- and lyosomes (stage C), cytosolic entry of the contrast agents (stage D), efflux of the contrast agents out of tumor cells (stage E), and washout of the agents out of the tumor region via the vascular system (stage F). Using this methodology, they convincingly showed that it is not only possible to noninvasively assess content release from nanocarrier materials using multicontrast MRI but also to visualize and analyze (the kinetics of) cellular uptake and cellular trafficking.

Another interesting method to visualize drug release from theranostic nanomedicine formulations has recently been published by Onuki and colleagues, who prepared poly(lactic-*co*-glycolic acid) (PLGA)-based nanoparticles carrying the drug 5-fluorouracil and the contrast agents gadolinium-DTPA (Gd-DTPA) and superparamagnetic iron oxide (SPIO).[23] They found that, immediately upon i.v. administration, the nanoparticles exhibited a strong T_2* contrast in the tumor area, as a result of the presence of the SPIO, which remained unaltered up until 2.5 h p.i. Conversely, T_1 mapping, which correlates to the release of Gd-DTPA from the SPIO-containing nanoparticles, only revealed a clear signal at 30 min p.i. This indicates that the release of Gd-DTPA, and likely also of co-loaded 5-FU, occurs relatively early on after i.v. administration, that is, already to a significant extent within 30 min, and that after this, the released low-molecular-weight gadolinium complex diffuses away relatively fast, as evidenced by the fact that the T1 signal had vanished at 2.5 h p.i. This is exemplified by the composite image in Figure 3G and H, which shows Gd-DTPA release (in red and yellow) at 30 min p.i., overlaid on the dark T_2*-enhanced signals coming from the SPIO-loaded nanoparticles. Assuming that 5-FU is released from these particles with the same kinetics as is Gd-DTPA (which still needs to be validated), this setup thus enables the simultaneous and quantitative monitoring of drug delivery and drug release.

Imaging Drug Efficacy

Besides for noninvasively assessing drug delivery and drug release, theranostic nanomedicines are also highly useful for predicting and monitoring therapeutic responses. Concerning the prediction of therapeutic responses, as already briefly alluded to above, during phase I and phase II clinical trials, nanomedicine formulations could, for instance, be labeled with radionuclides, in order to obtain some initial noninvasive information with regard to target site accumulation. On the basis of this, rational predictions could then be made with regard to the potential effectiveness of nanomedicine-based therapeutic interventions. In the initial phase I trial focusing on HPMA-copolymer-based doxorubicin (i.e., PK1), for instance, a radiolabeled version of this passively tumor-targeted polymeric prodrug could have been used to prescreen patients assigned to PK1, in order to identify which tumors are amenable to EPR-mediated drug targeting and which are not, and to thereby predict which patients are likely to respond to PK1 therapy and which are not. Similarly, in the phase I/II trial focusing on liver-targeted PK1 (i.e., PK2), the combination of functional SPECT imaging and anatomical CT imaging could have been used to visualize which HCC-patients show good tumor accumulation and which do not, and to on the basis of this decide in which patients PK2 treatment should be continued. Furthermore, by mixing in trace amounts of radiolabeled nanomedicines with (e.g., every second or third cycle of) drug treatment and by continuously subjecting patients to anatomical CT imaging in conjunction with 2D-scintigraphy or 3D-PET, it would have been possible to visualize the efficacy of the intervention in real-time, and to thereby provide important information for assisting in deciding whether or not to (dis)continue therapy, and whether or not to adjust drug doses. By doing so, theranostic nanomedicines might contribute to realizing the potential of "personalized medicine", that is, tailor-made therapy for individual patients, which, besides on the study of genetic polymorphisms and biomarkers, also relies on the development of imaging methods for predicting and measuring therapeutic responses.

Additional proof-of-principle for the use of theranostic nanomedicines for predicting and monitoring therapeutic responses is depicted in Figure 3I–L. Analogous to the efforts

mentioned above for PK1 and PK2, Figure 3K shows the accumulation of radiolabeled PEGylated liposomes in a patient suffering from AIDS-related Kaposi sarcoma.[13] Kaposi sarcomas (KS) are characterized by a dense and highly leaky vasculature, and long-circulating and passively tumor-targeted nanomedicines very effectively accumulate in these lesions by means of EPR. Consequently, KS patients generally respond very well to treatment with PEGylated liposomal doxorubicin (i.e., Doxil/Caelyx), and as opposed to other types of malignancy for which Doxil is approved, not only the tolerability of the intervention can be substantially improved, but also its efficacy: in a large phase III trial in which Doxil was compared to the formerly standard combination regimen ABV (i.e., adriamycin (doxorubicin), bleomycin, and vincristine), it was found that Doxil produced 1 complete response and 60 partial responses, as compared to only 31 partial responses for ABV.[24] This highly significant improvement in therapeutic efficacy can be explained by the fact that Doxil accumulates very well in KS lesions (Figure 3K), whereas in other types of malignancies its target site accumulation tends to be less effective and varies substantially from patient to patient (see Figure 4I). Following up on this and the above reasoning, if also KS and non-KS patients would be prescreened with radiolabeled Doxil, in order to identify which ones show high tumor accumulation and which ones do not, it would also in these cases be possible to decide in which patients Doxil treatment should be continued and in which ones other therapeutic options should be considered. The same holds true for adding in minute amounts of radiolabeled Doxil with (e.g., every second cycle of) drug treatment, to be able noninvasively visualize the efficacy of the intervention during follow-up, and to thereby assist in deciding whether or not to (dis)-continue therapy and whether or not to adjust drug doses. It should be kept in mind in this regard, however, that the in vivo visualization of the biodistribution and the target site accumulation of theranostic nanomedicines is an add-on parameter for providing feedback on the potential therapeutic efficacy of the intervention, and that it by no means replaces established (PET-, MR- or CT-based) diagnostic procedures.

Theranostic nanomedicines could furthermore also be used to noninvasively assess treatment efficacy in the case of antiangiogenic and antimetastatic treatments. Regarding antiangiogenic therapy, for instance, it has already been demonstrated that, by conjugating the highly putative antiangiogenic agent TNP-470 to HPMA copolymers, the balance between the efficacy and the toxicity of this drug can be substantially improved.[25] On the other hand, gadolinium-labeled HPMA copolymers have on various occasions been shown to circulate for prolonged periods of time and, consequently, to hold significant potential for experimental MR angiography.[26,27] This is exemplified in Figure 3L, showing that a 25 kDa-sized gadolinium-labeled HPMA copolymer can be used to visualize blood vessels in subcutaneous rat tumors with relatively high resolution. When combining the two above approaches, that is, by synthesizing a theranostic polymer therapeutic containing both TNP-470 and gadolinium, it would be possible to at the same induce and monitor antiangiogenesis.

Regarding metastasis, the images in Figure 3I–K exemplify that theranostic nanomedicine formulations are also highly useful for noninvasively assessing the antimetastatic efficacy of targeted therapeutic interventions. Figure 3I and J shows the accumulation of gadolinium-labeled polypropylene diaminobutane-based dendrimers in a healthy and in a metastatic mouse liver, respectively, and clearly demonstrates the suitability of these nanomedicine materials to visualize metastatic liver lesions.[28] Figure 3K shows a KS patient with various metastatic lesions in the upper left leg and in the right shoulder region, and demonstrates that also in this case, that is, upon co-loading liposomes both with drugs and with imaging agents, and upon adding in trace amount of radiolabeled liposomes with (e.g., every second or third cycle of) of Doxil treatment, the antimetastatic efficacy of the intervention can be noninvasively visualized in real-time.[13]

Conclusions

Theranostic nanomedicines can be used for various different purposes. By enabling a noninvasive assessment of the pharmacokinetics, the biodistribution and the target site localization of conjugated or entrapped pharmacologically active agents, nanotheranostics allow for the optimization of drug delivery systems. In addition, by combining information on overall target site localization with noninvasive imaging insights on the local distribution of the drug and/or the carrier material at the target site, nanotheranostics can also be used for predicting treatment responses. This is exemplified by the above-mentioned clinical studies on the tumor accumulation of radiolabeled PEGylated liposomes in Kaposi sarcoma patients, as well as by the liver versus tumor localization of galactosamine-targeted HPMA copolymers carrying doxorubicin. Furthermore, by noninvasively imaging (the kinetics of) drug release in vivo, some of the basic properties of drug delivery systems can be

visualized and analyzed, and attempts can be made to correlate the in vitro characteristics of carrier materials with their in vivo capabilities. Related to this, by using contrast agents to monitor the release of pharmacologically active agents from stimuli-sensitive nanomedicines, the efficacy of triggerable drug delivery systems can be optimized, as exemplified by several studies on thermosensitive liposomes. And finally, by providing real-time feedback on the efficacy of targeted therapeutic interventions, theranostic nanomedicines can also be used to facilitate (pre-) clinical efficacy analysis, to prescreen patients, and to realize the potential of personalized medicine.

BIOGRAPHICAL INFORMATION

Twan Lammers obtained a D.Sc. degree in Radiation Oncology from Heidelberg University in 2008, and a Ph.D. degree in Pharmaceutics from Utrecht University in 2009. Since 2007, he has been appointed as a postdoctoral fellow at the Department of Pharmaceutics at Utrecht University, and since 2009 as a group leader at the Department of Experimental Molecular Imaging at the Helmholtz Institute for Biomedical Engineering and the University of Aachen (RWTH). His primary research interests include drug targeting to tumors, image-guided drug delivery, and tumor-targeted combination therapies.

Silvio Aime is professor of General and Inorganic Chemistry and head of the Center of Molecular Imaging at the University of Torino. His research interests are centered around the development of targeting and responsive MRI agents for in vivo imaging investigations (early diagnoses, monitoring of therapeutic effects, visualization of drug delivery, and cellular therapy).

Wim E. Hennink obtained his Ph.D. degree in 1985 at the Twente University of Technology, on a thesis on a biomaterials topic. From 1985 until 1992 he had different positions in the industry. In 1992, he was appointed as professor at the Faculty of Pharmacy of the University of Utrecht. From 1996 onwards, he has been head of the Department of Pharmaceutics. His main research interests are in the field of polymeric drug delivery systems.

Gert Storm obtained his Ph.D. degree in Pharmaceutics at the University of Utrecht in 1987. He subsequently worked as a visiting scientist at Liposome Technology Inc. in Menlo Park, and as a visiting assistant professor at the School of Pharmacy at UCSF. Since 1991, he has been appointed at the University of Utrecht, where he became professor in 2000 (Drug Targeting chair). Since 2009, he also holds an honorary professorship at the Royal School of Pharmacy in Copenhagen (Biomacromolecular Drug Delivery).

Fabian Kiessling completed his M.D. thesis at Heidelberg University in 2001. He subsequently worked at the Departments of Radiology and Medical Physics in Radiology at the German Cancer Research Center in Heidelberg, where he headed the Molecular Imaging Group. Since 2008, he is the chair of the Department of Experimental Molecular Imaging at the Helmholtz Institute for Biomedical Engineering and the University of Aachen (RWTH). With a particular focus on angiogenesis, the aim of his research is the development of novel diagnostic probes and imaging tools for disease-specific diagnosis and therapy monitoring.

The authors gratefully acknowledge financial support by High-tech.NRW (ForSaTum) and by the European Commission's Framework Programme (FP6: "MediTrans - Targeted Delivery of Nanomedicines"; and FP7: "COST-Action TD1004: Theragnostics for imaging and therapy - An action to develop novel nanosized systems for imaging-guided drug delivery").

FOOTNOTES

*To whom correspondence should be addressed. E-mail: tlammers@ukaachen.de, t.lammers@uu.nl.
⊥Shared senior authorship.

REFERENCES

1 Peer, D.; Karp, J. M.; Hong, S.; Farokhzad, O.; Margalit, R.; Langer, R. Nanocarriers as an emerging platform for cancer therapy. *Nat. Nanotechnol.* **2007**, *2*, 751–760.
2 Sanhai, W. R.; Sakamoto, J. H.; Canady, R.; Ferrari, M. Seven challenges for nanomedicine. *Nat. Nanotechnol.* **2008**, *3*, 242–244.
3 Davis, M. E.; Chen, Z. G.; Shin, D. M. Nanoparticle therapeutics: an emerging treatment modality for cancer. *Nat. Rev. Drug Discovery* **2008**, *7*, 771–782.
4 Lammers, T.; Hennink, W. E.; Storm, G. Tumour-targeted nanomedicines: principles and practice. *Br. J. Cancer* **2008**, *99*, 392–397.
5 Caruthers, S. D.; Wickline, S. A.; Lanza, G. M. Nanotechnological applications in medicine. *Curr. Opin. Biotechnol.* **2007**, *18*, 26–30.
6 Xie, J.; Lee, S.; Chen, X. Nanoparticle-based theranostic agents. *Adv. Drug Delivery Rev.* **2010**, *62*, 1064–1079.
7 Sun, D. Nanotheranostics: integration of imaging and targeted drug delivery. *Mol. Pharmaceutics* **2010**, *7*, 1879.
8 Lammers, T.; Kiessling, F.; Hennink, W. E.; Storm, G. Nanotheranostics and image-guided drug delivery: Current concepts and future directions. *Mol. Pharmaceutics* **2010**, *7*, 1899–1912.
9 Maeda, H.; Wu, J.; Sawa, T.; Matsumura, Y.; Hori, K. Tumour vascular permeability and the EPR effect in macromolecular therapeutics: a review. *J. Controlled Release* **2000**, *65*, 271–284.
10 Lammers, T.; Subr, V.; Ulbrich, K.; Hennink, W. E.; Storm, G.; Kiessling, F. Polymeric nanomedicines for image-guided drug delivery and tumor-targeted combination therapy. *Nano Today* **2010**, *5*, 197–212.
11 Lammers, T.; Kuehnlein, R.; Kissel, M.; Subr, V.; Etrych, T.; Pola, R.; Pechar, M.; Ulbrich, K.; Storm, G.; Huber, P.; Peschke, P. Effect of physicochemical modification on the biodistribution and tumor accumulation of HPMA copolymers. *J. Controlled Release* **2005**, *110*, 103–118.
12 Seymour, L. W.; Ferry, D. R.; Anderson, D.; Hesslewood, S.; Julyan, P. J.; Poyner, R.; Doran, J.; Young, A. M.; Burtles, S.; Kerr, D. J. Hepatic drug targeting: phase I evaluation of polymer-bound doxorubicin. *J. Clin. Oncol.* **2002**, *20*, 1668–1676.
13 Harrington, K. J.; Mohammadtaghi, S.; Uster, P. S.; Glass, D.; Peters, A. M.; Vile, R. G.; Stewart, J. S. Effective targeting of solid tumors in patients with locally advanced cancers by radiolabeled pegylated liposomes. *Clin. Cancer Res.* **2001**, *7*, 243–254.
14 Lammers, T.; Subr, V.; Ulbrich, K.; Peschke, P.; Huber, P. E.; Hennink, W. E.; Storm, G. Simultaneous delivery of doxorubicin and gemcitabine to tumors in vivo using prototypic polymeric drug carriers. *Biomaterials* **2009**, *30*, 3466–3475.
15 Dams, E. T.; Laverman, P.; Oyen, W. J.; Storm, G.; Scherphof, G. L.; van Der Meer, J. W.; Corstens, F. H.; Boerman, O. C. Accelerated blood clearance and altered biodistribution of repeated injections of sterically stabilized liposomes. *J. Pharmacol. Exp. Ther.* **2000**, *292*, 1071–1079.
16 Viglianti, B. L.; Abraham, S. A.; Michelich, C. R.; Yarmolenko, P. S.; MacFall, J. R.; Bally, M. B; Dewhirst, M. W. In vivo monitoring of tissue pharmacokinetics of liposome/drug using MRI: illustration of targeted delivery. *Magn. Reson. Med.* **2004**, *51*, 1153–1162.
17 Viglianti, B. L.; Ponce, A. M.; Michelich, C. R.; Yu, D.; Abraham, S. A.; Sanders, L.; Yarmolenko, P. S.; Schroeder, T.; MacFall, J. R.; Barboriak, D. P.; Colvin, O. M.; Bally, M. B.; Dewhirst, M. W. Chemodosimetry of in vivo tumor liposomal drug concentration using MRI. *Magn. Reson. Med.* **2006**, *56*, 1011–1018.
18 De Smet, M.; Heijman, E.; Langereis, S.; Hijnen, N. M.; Grüll, H. Magnetic resonance imaging of high intensity focused ultrasound mediated drug delivery from

temperature-sensitive liposomes: An in vivo proof-of-concept study. *J. Controlled Release* **2011**, *150*, 102–110.

19 Negussie, A. H.; Yarmolenko, P. S.; Partanen, A.; Ranjan, A.; Jacobs, G.; Woods, D.; Bryant, H.; Thomasson, D.; Dewhirst, M. W.; Wood, B. J; Dreher, M. R. Formulation and characterisation of magnetic resonance imageable thermally sensitive liposomes for use with magnetic resonance-guided high intensity focused ultrasound. *Int. J. Hyperthermia* **2011**, *27*, 140–155.

20 Langereis, S.; Keupp, J.; van Velthoven, J. L.; de Roos, I. H.; Burdinski, D.; Pikkemaat, J. A.; Gruell, H. A temperature-sensitive liposomal 1H CEST and 19F contrast agent for MR image-guided drug delivery. *J. Am. Chem. Soc.* **2009**, *131*, 1380–1381.

21 Deckers, R.; Moonen, C. T. Ultrasound triggered, image guided, local drug delivery. *J. Controlled Release* **2010**, *148*, 25–33.

22 Delli Castelli, D.; Dastru, W.; Terreno, E.; Cittadino, E.; Mainini, F.; Torres, E.; Spadaro, M.; Aime, S. In vivo MRI multicontrast kinetic analysis of the uptake and intracellular trafficking of paramagnetically labeled liposomes. *J. Controlled Release* **2010**, *144*, 271–279.

23 Onuki, Y.; Jacobs, I.; Artemov, D.; Kato, Y. Noninvasive visualization of in vivo release and intratumoral distribution of surrogate MR contrast agent using the dual MR contrast technique. *Biomaterials* **2010**, *31*, 7132–7138.

24 Northfelt, D. W.; Dezube, B. J.; Thommes, J. A.; Miller, B. J.; Fischl, M. A.; Friedman-Kien, A.; Kaplan, L. D.; Du Mond, C.; Mamelok, R. D.; Henry, D. H. Pegylated-liposomal doxorubicin versus doxorubicin, bleomycin, and vincristine in the treatment of AIDS-related Kaposi's sarcoma: results of a randomized phase III clinical trial. *J. Clin. Oncol.* **2005**, *16*, 2445–2451.

25 Satchi-Fainaro, R.; Puder, M.; Davies, J. W.; Tran, H. T.; Sampson, D. A.; Greene, A. K.; Corfas, G.; Folkman, J. Targeting angiogenesis with a conjugate of HPMA copolymer and TNP-470. *Nat. Med.* **2004**, *10*, 255–261.

26 Kiessling, F.; Heilmann, M.; Lammers, T.; Ulbrich, K.; Subr, V.; Peschke, P.; Waengler, B.; Mier, W.; Schrenk, H. H.; Bock, M.; Schad, L.; Semmler, W. Synthesis and characterization of HE-24.8: a polymeric contrast agent for magnetic resonance angiography. *Bioconjugate Chem.* **2006**, *17*, 42–51.

27 Lammers, T.; Subr, V.; Peschke, P.; Kuehnlein, R.; Hennink, W. E.; Ulbrich, K.; Kiessling, F.; Heilmann, M.; Debus, J.; Huber, P. E.; Storm, G. Image-guided and passively tumour-targeted polymeric nanomedicines for radiochemotherapy. *Br. J. Cancer* **2008**, *99*, 900–910.

28 Kobayashi, H.; Brechbiel, M. W. Nano-sized MRI contrast agents with dendrimer cores. *Adv. Drug Delivery Rev.* **2005**, *57*, 2271–2286.